

Liquid ordering at the Brushite- $\{010\}$ -water interface

J. Arsic, D. Kaminski, P. Poodt, and E. Vlieg*

NSRIM Department of Solid State Chemistry, University of Nijmegen, Toernooiveld 1, 6525 ED Nijmegen, The Netherlands

(Received 15 August 2003; revised manuscript received 26 February 2004; published 21 June 2004)

Using surface x-ray diffraction, we have determined the atomic structure of the $\{010\}$ interface of brushite, $\text{CaHPO}_4 \cdot 2(\text{H}_2\text{O})$, with water. Since this biomineral contains water layers as part of its crystal structure, special ordering properties at the interface are expected. We found that this interface consists of two water bilayers with different ordering properties. The first water bilayer is highly ordered and can be considered as part of the brushite crystal structure. Surprisingly, the second water bilayer exhibits no in-plane order, but shows only layering in the perpendicular direction. We propose that the low level of water ordering at the interface is correlated with the low solubility of brushite in water.

DOI: 10.1103/PhysRevB.69.245406

PACS number(s): 68.08.De, 87.68.+z

A proper understanding of physical and chemical phenomena such as crystal growth from solution, lubrication, and electrochemistry requires structural knowledge of the solid-liquid interface at an atomic scale. For a long time suitable experimental techniques were not available and the main ideas were derived from theoretical models^{1,2}. Such theoretical studies made it clear that the first few liquid layers in contact with the crystal surface have special properties. The liquid near the interface is influenced by the periodic potential of the crystal surface and is expected to show more ordering than in the bulk liquid. The ordering is predicted to be stronger in the perpendicular than in the lateral direction. Layering of the liquid in the direction perpendicular to the surface has indeed been observed in a few cases. Toney *et al.*³ showed layering of the liquid at an electrode/electrolyte interface as a function of voltage. Huisman *et al.*⁴ found evidence for layering of liquid gallium in contact with a diamond surface using x-ray diffraction. Recently Cheng *et al.*⁵ found molecular-scale density oscillation at the water/mica interface using specular reflectivity.

Detecting the amount of in-plane ordering of the liquid has proven to be even more difficult. It has been observed in simple model systems consisting of Pb and Sn monolayers on a Ge(111) surface⁶⁻⁸. Using transmission electron microscopy, lateral ordering was observed qualitatively in thicker films.⁹ Recently, a single icelike layer was found at the RuO_2 -water interface,¹⁰ and we derived the complete ordering components of a potassium dihydrogen phosphate (KDP) $\{101\}$ surface in contact with water.¹¹ From these studies the picture emerges that a liquid in contact with a crystal surface has both solid and liquid properties. The transition to bulk liquid behavior appears to depend strongly on the particular system. At the RuO_2 -water interface lateral ordering seems absent beyond the first layer, while in the case of KDP the first three water layers show varying degrees of lateral order. The structure of single water layers, with a particular emphasis on $\text{Ru}(0001)$ at low temperatures, has been a controversial topic for many years, but either the specific systems studied or the technique used make the results less relevant for the type of water-solid interfaces discussed here.^{12,13}

In order to gain a better understanding of the water ordering at interfaces, we determined the structure of the brushite- $\{010\}$ -water interface. This crystal is one of the major com-

ponents of kidney stones and has a wide use as a coating for bone implants. Brushite, also known as DCPD [dicalcium hydrogenphosphate dihydrate, $\text{CaHPO}_4 \cdot 2(\text{H}_2\text{O})$], is a model system for biomineralization. It grows easily from solution in a platelike morphology. Although the growth and surface structure of brushite single crystals have been studied,^{14,15} the interface atomic structure of the most prominent faces has not been determined. The property that makes this crystal particularly attractive for the investigation of solid-liquid interfaces is that brushite has water ("ice") incorporated in the crystal structure. These water layers appear as bilayers parallel to the $\{010\}$ orientation, as shown in Fig. 1. Owing to the ordered water in the crystal structure of brushite, liquid ordering at the interface is expected to be quite strong. However, to our surprise, we found the water ordering to be weaker for brushite than for KDP.

Single brushite crystals of $2 \times 4 \times 0.5 \text{ mm}^3$ in size were isolated from the agarose gel growth medium by washing

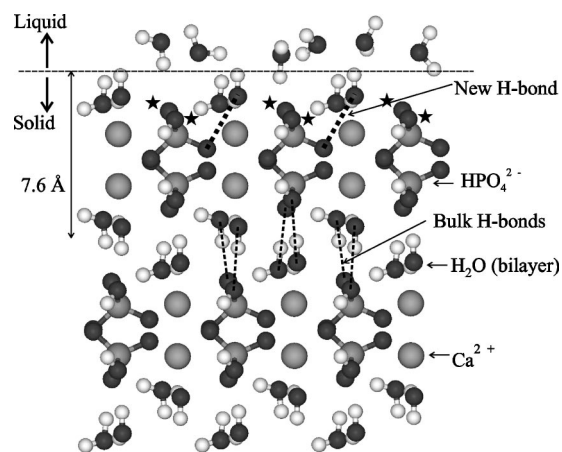


FIG. 1. Schematic side view of the $\{010\}$ face of $\text{CaHPO}_4 \cdot 2(\text{H}_2\text{O})$. The water is incorporated as two bilayers. Some of the hydrogen bonds in the bulk are represented with dashed lines. Stars indicate locations where the hydrogen bonds are broken due to the surface termination. The dashed lines at the surface indicate possible new hydrogen bonds owing to the surface relaxation. The hydrogen positions in the top layers (and especially in the liquid layer) are only an impression because these cannot be derived from the present x-ray diffraction data.

them with pure ethanol. Using atomic force microscopy (AFM), we found the brushite surface to be flat and covered with monoatomic steps. The step height of 7.6 Å agrees with previous results¹⁵ and corresponds to half a unit cell in the $\langle 010 \rangle$ direction. The bulk crystal structure (Fig. 1) allows several surface terminations of the $\{010\}$ face: single or double layers of either water or calcium phosphate. The constant step height proves that only one termination is realized.

We performed surface x-ray diffraction experiments at the ID03 beam line of the European Synchrotron Radiation Facility (ESRF) in Grenoble using an x-ray energy of 10 keV. This is one of the few techniques that can be applied for the structure determination in nonvacuum environments.¹⁶ In order to obtain data with the required accuracy, the water layer has to be very thin, because otherwise the background signal becomes too high.¹¹ We therefore exploited the fact that in a humid environment the crystal is covered by a thin water layer. The experimental setup consists of a sample environmental chamber¹⁷ that was coupled to a z -axis diffractometer and that can operate in different modes from dry to 100% humidity. The environmental chamber was mounted on the diffractometer in such a way that the crystal $\{010\}$ surface was in the horizontal plane.

We found that the x rays induced severe beam damage in the bulk crystal, which leads to a huge background intensity and also to surface roughness. The effect was found to depend on the measuring conditions and was not linear in the beam intensity. In air a surface lasted only about 20 s in the full x-ray beam. The damage could be minimized by measuring at 100% humidity and with the beam intensity reduced by a factor of 30. In this way an equilibrium between damage and healing of the surface seems to be established. We thus present below only data measured under these optimum conditions.

In order to denote the brushite $\{010\}$ surface, we define a unit cell with lattice vectors $\{\mathbf{a}_i\}$, which can be expressed in terms of the conventional monoclinic lattice vectors ($a = 5.812$ Å, $b = 15.18$ Å, and $c = 6.239$ Å) as

$$\begin{aligned} \mathbf{a}_1 &= [001]_{\text{monoclinic}}, \quad \mathbf{a}_2 = [100]_{\text{monoclinic}}, \quad \text{and} \quad \mathbf{a}_3 \\ &= [010]_{\text{monoclinic}}. \end{aligned}$$

The reciprocal lattice vectors \mathbf{b}_i are defined by $\mathbf{a}_i \cdot \mathbf{b}_j = 2\pi\delta_{ij}$. The momentum transfer vector \mathbf{Q} , which is the difference between the wave vectors of the incident and scattered x rays, is then $\mathbf{Q} = h\mathbf{b}_1 + k\mathbf{b}_2 + l\mathbf{b}_3$, with (hkl) the diffraction indices. Here, the reciprocal lattice vectors are chosen such that the diffraction index l denotes the perpendicular component of \mathbf{Q} .

For a flat crystal surface, there is a continuous intensity distribution along the l direction, the so-called crystal truncation rods (CTR's).¹⁸ These rods are tails of diffuse intensity connecting the bulk Bragg peaks in the direction perpendicular to the surface. Their exact shape is determined by the interface atomic structure. Integrated intensities of various reflections were determined by rocking the crystal and measuring the number of diffracted photons. The integrated intensities were converted into structure factor amplitudes by

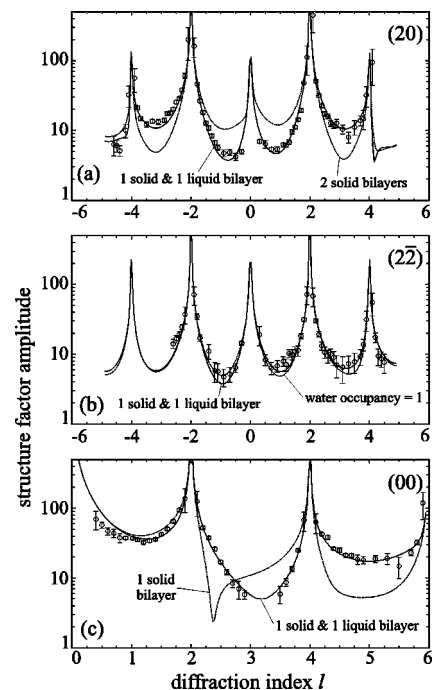


FIG. 2. The structure factor amplitude along the (20) , $(2\bar{2})$, and (00) rods. Open circles represent the data points, solid curves the best fit with two adsorbed water bilayers (as described in the text). The dashed curve in (a) represents a model calculation for a termination with two completely ordered water bilayers; in (b) the dotted curve is for a model in which the occupancy in the surface water bilayers is forced to be equal to 1; in (c) the dash-dotted curve represents a termination with only one completely ordered water bilayer.

applying the necessary geometrical and resolution corrections.¹⁹ Model calculations and fitting were done using the ROD code, using χ^2 as goodness-of-fit criterion.²⁰

We measured in total 155 nonequivalent reflections, consisting of the (00) (or specular), (20) and $(2\bar{2})$ rods, with an agreement factor of 8% when averaged over all different samples used.²¹ The data are shown in Fig. 2. We did not search for surface reconstructions, since AFM shows that these are not present.¹⁵ In order to fully determine the liquid ordering, it is crucial to measure rods with different in-plane momentum transfer.¹¹ The specular rod is only sensitive to the electron density perpendicular to the surface and ignores in-plane order. The other rods probe the lateral order as well. Since the ordering is strongest in the perpendicular direction, the specular rod will probe more liquid layers than the other rods.

For a proper fitting of the data we need a model that describes the entire interface, both the crystalline brushite surface and the partially ordered water. The water layers of the interface are modeled as complete bilayers, just as they appear in the brushite bulk structure (see Fig. 1). This approach proved to be the best after an extensive analysis of different models for the liquid part of the interface. For example, including a separate treatment of the upper and lower half of a bilayer was not meaningful given the size of the data set. Because x-rays are very insensitive to hydrogen

TABLE I. Best fit parameters for the water bilayers. The (fixed) high DW_{\parallel} value for layer 2 means that this has no in-plane order. The relaxation is indicated with respect to bulk-extrapolated positions. The occupancy is relative to a bulk crystal.

	z displacement (\AA)	$DW_{\parallel}(\text{\AA}^2)$	$DW_{\perp}(\text{\AA}^2)$	Occupancy
Bilayer 2	0.3 ± 0.1	500	0.6 ± 0.4	1.6 ± 0.4
Bilayer 1	-0.15 ± 0.1	4 ± 2	0.6 ± 0.4	1.6 ± 0.4

atoms, these are kept at the same orientation with respect to the associated oxygen atoms as in the bulk crystal. The amount of ordering of each water bilayer is fitted through anisotropic Debye-Waller (DW) parameters. A small in-plane DW parameter corresponds to a layer with high lateral ordering that will contribute to all rods. Liquid layers that contribute only to the specular rod are modeled by giving them a fixed, large in-plane DW parameter of 500\AA^2 . The occupancy of the water layers is also fitted, because the density at the interface may be different from exactly one bilayer per unit cell. Other fitting parameters used were surface roughness, a scale factor, and relaxation of the top water layers.

We first need to address the termination of the crystal. This is most easily determined using the rods that are sensitive to the in-plane order. We find in this way that the crystal terminates with a single water bilayer. This fit is shown by the solid curve in Fig. 2(a). Other terminations did not yield a satisfactory fit ($\chi^2 > 14$). The dashed line in Fig. 2(a) is, for example, a calculation with two fully ordered water bilayers at the interface. A model with one bilayer, however, does not give a good fit for the specular rod, as represented by the dash-dotted curve in Fig. 2(c). We find that we can only fit the specular rod if an extra water layer is added. The specular rod thus “sees” *two* water layers, the other rods only *one*. Adding more laterally disordered water layers leads to a minor improvement of the specular fit, but does not significantly change the parameters of the first two water bilayers. The full model therefore consists of one highly ordered water bilayer and one additional bilayer without in-plane ordering. This model describes all our data well, yielding a χ^2 of 2.9 for the entire data set, and it is represented by the solid curves in Fig. 2. The best fitting parameters are given in Table I. Relaxation of the top calcium and phosphate layers was found to be negligible. The first water bilayer relaxes inward by 0.15\AA , while the distance between layers 1 and 2 is 0.5\AA larger than in the bulk. The first water bilayer has an enhanced in-plane DW parameter.

Under our measuring conditions, the total water thickness is limited to 2 or 3 layers. We expect very similar properties for the interfacial water layers if a geometry with a thicker water film would have been used, since the lateral ordering is found to be restricted to a single layer. In particular, the fact that the second water layer shows no lateral ordering should not change if more water layers are present.

Our best fit indicates an enhanced occupancy (density) of the first two water bilayers. The extra water molecules would have to be located at different sites, because an occupancy of 1 means that all bulk sites are occupied. Our data set, however, does not allow such structural details to be extracted.

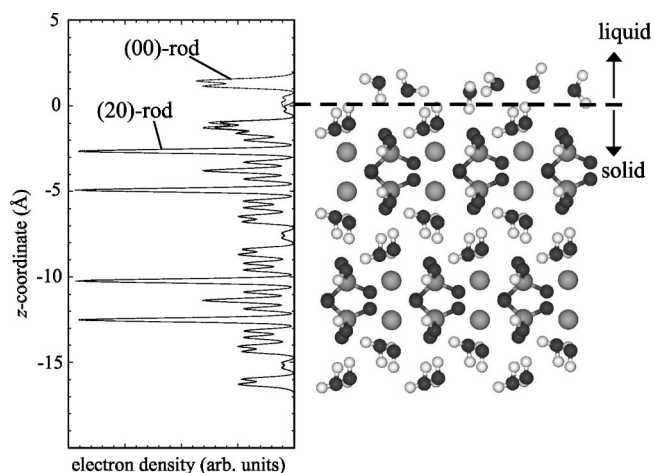


FIG. 3. Schematic side view of the $\{010\}$ face of $\text{CaHPO}_4 \cdot 2(\text{H}_2\text{O})$ (right) together with the electron density distribution across the interface determined from two different rods (left). The (00) rod yields the genuine distribution, including the laterally disordered layer. Relaxation in the water bilayers is included.

Since the occupancy is correlated with the DW parameters, the error bars on the enhanced occupancy are quite large. Forcing the occupancy in both bilayers to be equal to 1 leads to $\chi^2 = 3.7$. The dotted line in Fig. 2(b) shows the result of this fit for the $(2\bar{2})$ rod. Figure 2 clearly shows that the data are far more sensitive to the difference between order and disorder than to the occupancy. If the “ice density” in bulk brushite is defined by using the water bilayer separation as the layer separation in an imaginary crystal consisting of a stack of such layers, the density is only 4% higher than in normal ice I_h . An increase by 60% (as indicated by the enhanced occupancies) seems therefore unlikely, even though the interface may deviate from the bulk. The other fitting parameters (and in particular the ordering) fortunately depend only weakly on the specific values for the occupancy.

A convenient way to visualize the properties of the water layer is by calculating the projection of the electron density distribution along the z axis. The in-plane order of the water can be taken into account using an additional term in the density distribution depending on the in-plane momentum transfer and in-plane DW parameters.¹¹ The electron density distribution for the specular rod is the genuine distribution, which includes the electron density of the water layers without in-plane order. The profiles for a nonspecular rod show the part of the electron density that corresponds to that Fourier component in the liquid. The results are given in Fig. 3 for the (00) and (20) rods and show that while the specular rod detects about two water bilayers, the other rods find only one bilayer with in-plane order. For clarity, the crystallographic structure is shown as well.

Due to the termination of the brushite- $\{010\}$ surface in one bilayer, two hydrogen bonds between phosphate groups and water in the second bilayer are broken. Stars in Fig. 1 indicate these bonds. The driving force for the inward relaxation of the crystalline water bilayer could therefore be the

formation of a compensating hydrogen bond with a lower lying phosphate group as represented by the dashed line in the top layer in Fig. 1. This is the only new O-O hydrogen bond with the expected distance near 2.73 Å. Some dynamic hydrogen bridges between layers 1 and 2 are expected to occur, but the enlarged separation of the layers indicates that these are not very important.

Our data show that water in contact with the brushite- $\{010\}$ surface shows less ordering than “expected,” in particular when compared with the water ordering at the KDP $\{101\}$ -water interface.¹¹ Water in contact with the positively charged KDP- $\{010\}$ surface shows icelike ordering in the first two water layers and weak but clear in-plane ordering in the third water layer. For the brushite system, which contains water layers in the crystal structure, less ordering is found. Apparently, liquid ordering is energetically less favorable in brushite than in KDP. We propose that the origin of this difference is the large difference in solubility. At room temperature, brushite is almost a thousand times less soluble in water than KDP. This occurs due to the special properties of the calcium ion.²² Less soluble means a weaker interaction with water, and thus less ordering at the interface. The RuO₂-water interface is the only other example in the literature studied in sufficient detail,¹⁰ and it combines low solubility with little ordering beyond an icelike layer. Recent results by us on NaCl(100) also support this proposed correlation between liquid order and solubility.²³

Ordered water at the brushite interface will influence the growth process of this biomineral, particularly the incorporation of the growth units at step edges and the mobility at the interface. Furthermore, the knowledge of the surface structure is needed to explain the influence of the impurities on the growth morphology.^{24,25} In biological mineralization, organic macromolecules are utilized to control the size, shape, and orientation of the crystals, the same properties that are of importance for creating good ceramic materials for production of artificial implants and other medical devices. We hope that our results on the most prominent crystal face of brushite will help to develop the controlled growth of this important biomineral.

The authors would like to thank the staff of the beamline ID03 beam line at European Synchrotron Radiation Facility in Grenoble, France, for their valuable assistance during the measurements. The help of Cristina Orme, Anna Villacampa, and Noriko Kanzaki in providing us with beautiful brushite samples is greatly appreciated. We thank Paul Verwer for assistance with Cerius², Neda Radenovic for help during AFM measurements, and Willem van Enckevort, Hugo Meekes, and Jim de Yoreo for inspiring discussions. This work is part of the research program of the Foundation for Fundamental Research on Matter (FOM) and was made possible by financial support from the Netherlands Organization for Scientific Research (NWO).

*Author to whom correspondence should be addressed. Electronic address: vlieg@sci.kun.nl

¹W. A. Curtin, Phys. Rev. Lett. **59**, 1228 (1987).

²F. Spaepen, Acta Metall. **23**, 729 (1975).

³M. F. Toney *et al.*, Nature (London) **368**, 444 (1994).

⁴W. J. Huisman *et al.*, Nature (London) **390**, 379 (1997).

⁵L. Cheng, P. Fenter, K. L. Nagy, M. L. Schlegel, and N. C. Sturchio, Phys. Rev. Lett. **87**, 156103 (2001).

⁶F. Grey, R. Feidenhans'l, J. S. Pedersen, M. Nielsen, and R. L. Johnson, Phys. Rev. B **41**, 9519 (1990).

⁷M. F. Reedijk, J. Arsic, F. K. de Theije, M. T. McBride, K. F. Peters, and E. Vlieg, Phys. Rev. B **64**, 033403 (2001).

⁸S. A. de Vries, P. Goedkindt, P. Steadman, and E. Vlieg, Phys. Rev. B **59**, 13 301 (1999).

⁹S. E. Donnelly *et al.*, Science **296**, 507 (2002).

¹⁰Y. S. Chu, T. E. Lister, W. G. Cullen, H. You, and Z. Nagy, Phys. Rev. Lett. **86**, 3364 (2001).

¹¹M. F. Reedijk, J. Arsic, F. F. A. Hollander, S. A. de Vries, and E. Vlieg, Phys. Rev. Lett. **90**, 066103 (2003).

¹²V. Sadtchenko, P. Conrad, and G. E. Ewing, J. Chem. Phys. **116**,

4293 (2002).

¹³A. Michaelides, A. Alavi, and D. A. King, J. Am. Chem. Soc. **125**, 2746 (2003).

¹⁴F. Abbona *et al.*, J. Cryst. Growth **131**, 331 (1993).

¹⁵N. Kanzaki *et al.*, J. Cryst. Growth **235**, 465 (2002).

¹⁶E. Vlieg, Surf. Sci. **500**, 458 (2002).

¹⁷M. F. Reedijk, Ph.D. thesis, University of Nijmegen, Nijmegen (2003).

¹⁸I. K. Robinson, Phys. Rev. B **33**, 3830 (1986).

¹⁹E. Vlieg, J. Appl. Crystallogr. **30**, 532 (1997).

²⁰E. Vlieg, J. Appl. Crystallogr. **33**, 401 (2000).

²¹I. K. Robinson, in *Handbook on Synchrotron Radiation*, edited by G. S. Brown and D. E. Moncton (North-Holland, Amsterdam, 1991), Vol. 3, p. 221.

²²A. T. Rutgers, Trans. Faraday Soc. **58**, 2184 (1962).

²³J. Arsic, D. M. Kaminski, N. Radenovic, P. Poodt, W. S. Graswinckel, H. M. Cuppen, and E. Vlieg, J. Chem. Phys. **120**, 9720 (2004).

²⁴S. A. de Vries *et al.*, Phys. Rev. Lett. **80**, 2229 (1998).

²⁵M. Sikiric *et al.*, Langmuir **16**, 9261 (2000).